CHAPTER II
LITERATURE SURVEY

2.1 Selective Diffusion of Gases through Solids

According to membrane-based separation processes, separations may be achieved by selectively passing (permeating) one or more components of a stream through a membrane while retarding the passage of one or more other components (Humphrey and Keller, 1997). Therefore, the composition of the material passing through the membrane is different from that not passing through. It is important to note that there are four different mechanisms, as shown in Figure 2.1;

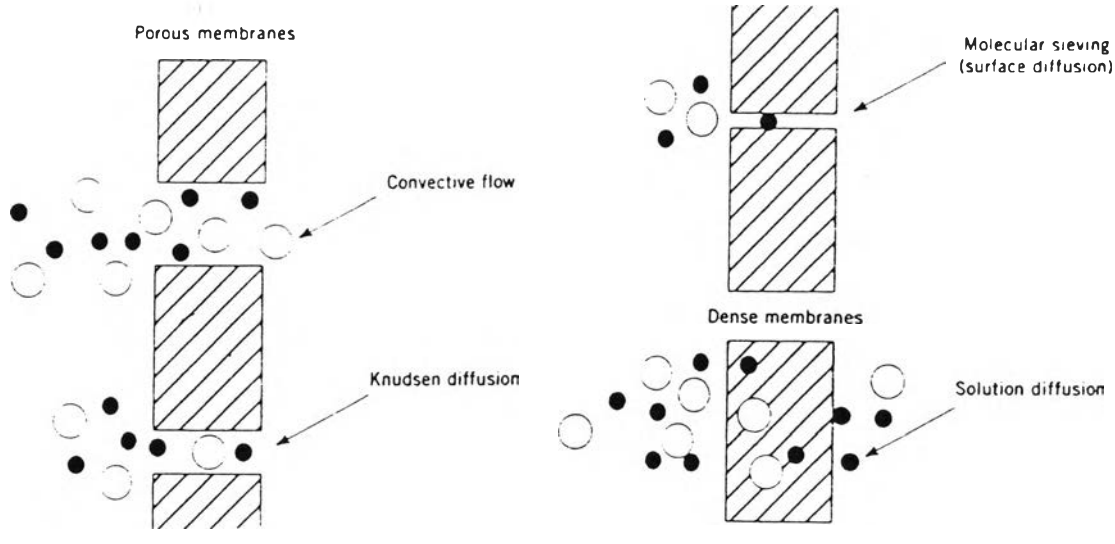

Figure 2.1 Mechanism for permeation of gases through porous and dense gas-separation polymer (Ruthen, 1997).

2.1.1 Diffusion Mechanism

2.1.1.1 Convective Flow

If the pores are relatively large, in the range 0.1-10 μm, gases permeate the membrane by convective flow, and there is no separation.

2.1.1.2 Knudsen Diffusion

If the pores are smaller than 0.1 μm, the pore diameter is the same size or smaller than mean free path of the gas molecules. Diffusion through such pores is governed by Knudsen diffusion. According to the Graham's law of diffusion, the permeation rate of different gases is inversely proportional to the square root of the molecular weight.

2.1.1.3 Molecular Sieving (Surface Diffusion)

If membrane pores are very small, of order 0.5-2 nm, then molecules are separated by molecular sieving. This molecular sieving is useful in separating molecules of different sizes. It is physically selective and hinges on the relative sizes of the diffusing species and the pore. This mechanism allows small molecules to pass through the porous medium but retards larger molecules, by having enough pores which are of such a size that the large molecules are unable to pass through.

2.1.1.4 Solution-Diffusion

This mechanism becomes operative, below 0.5 nm particle size such as permeation of gases through polymers when the driving force for transport is either concentration or pressure. Polymeric films in general can be regarded as interspersed crystalline and amorphous regions. The regular structure in crystalline region is assumed to be impermeable to liquids and gases. On the other hand, the polymer segments in the amorphous phase can have thermal motion and are able to be pushed aside to make space for permeated molecules.

The permeation process through a polymer material consists of three steps, as follows (Perry, 1984);

1. Solution of the permeant molecules at the upstream side of polymer
2. Diffusion of these molecules through the polymer
3. Desorption at the downstream side of polymer

Gas transport through dense polymers is governed by the following equation;

$$J_i = \frac{P_i (p_{i(0)} - p_{i(l)})}{l} \qquad (2.1)$$

$$\alpha_{ij} = \frac{P_i}{P_j} \qquad (2.2)$$

where J_i is the flux of component i.

$p_{i(o)}$ and $p_{i(l)}$ are the partial pressure of the component i on the either side of the polymer.

l is the polymer thickness.

P_i and P_j are constant called the membrane permeability of component i and j, respectively, which is a measure of the membrane 's ability to permeate gas.

α_i is the selectivity.

Permeability (P_i) can be expressed in terms of the diffusion coefficient (D_i) and the Henry's Law sorption coefficient or Henry's Law constant (S_i). The former reflects the mobility of the individual molecules in the polymer materials. The latter influences the number of molecules dissolved in the polymer materials. In order to identify the selectivity of a

polymer, equation (2.2) is modified and written as equation (2.3) (Winston and Sirkar, 1992).

$$\alpha_{ij} = \left[\frac{D_i}{D_j}\right]\left[\frac{S_i}{S_j}\right] \qquad (2.3)$$

The ratio D_i/D_j is the ratio of the diffusion coefficient which can be indicated as the mobility selectivity, reflecting the different sizes of two molecules. If the molecule i is larger than j, then the mobility selectivity will always be less than one. For all polymer materials, the diffusion coefficient decreases with increasing molecular size, since larger molecules interact with more segments of the polymer chain than do smaller molecules. Therefore, the mobility selectivity always favors the passage of small molecules over large ones. The magnitude of the mobility selectivity term is different for glassy and rubbery materials (see Figure 2.2). With increasing permeant size, diffusion coefficients in glassy materials decrease dramatically when compare to the diffusion coefficient in rubber, in which the polymer chain can rotate.

The ratio S_i/S_j is the ratio of the Henry's Law sorption coefficient which can be termed the sorption or solubility selectivity, reflecting the relative condensabilities of two gases. This ratio is normally greater than one, hence, larger molecules are more soluble than smaller ones. The sorption coefficient of gases or vapors, which is a measure of the energy required for the permeant to be sorbed by the polymer, increases with increasing condensability of the permeant and molecular diameter because large molecules are normally more condensable than smaller ones. The difference between the sorption coefficients of permeants in rubbery and glassy polymers is much less than those of the diffusion coefficients.

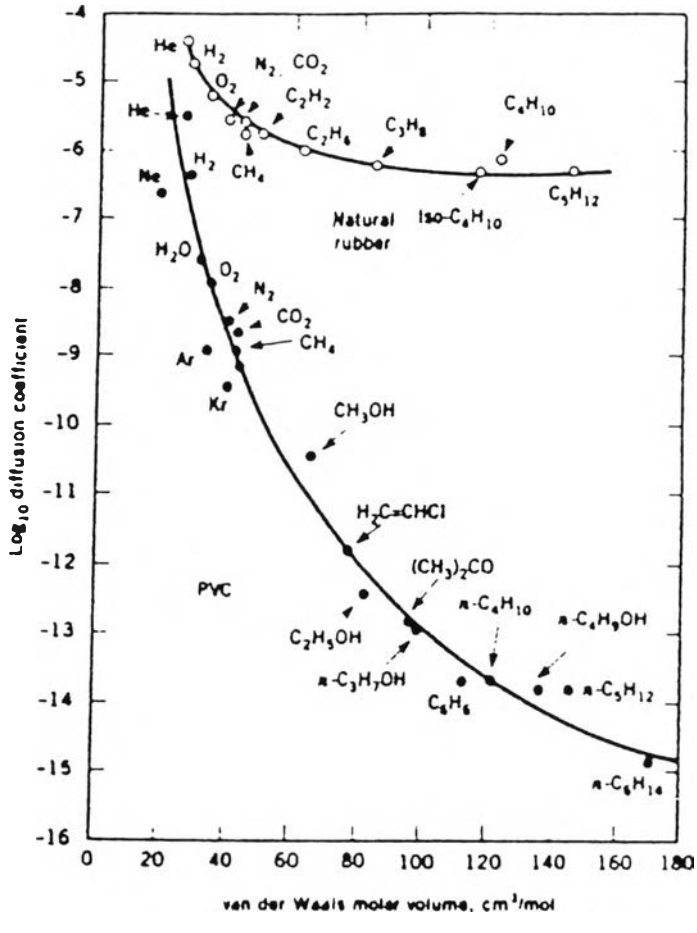

Figure 2.2 Diffusion Coefficient as a function of molar volume for a variety of permeants in natural rubber and in poly(vinyl chloride)(PVC)

In glassy polymers, the mobility term is usually dominant. The permeability drops with increasmg permeant size whereas the permeability increases with increasing permeant size. The larger molecules permeate preferentially in rubbery polymers, in which the sorption selectivity term is dominant. (see Figure 2.3).

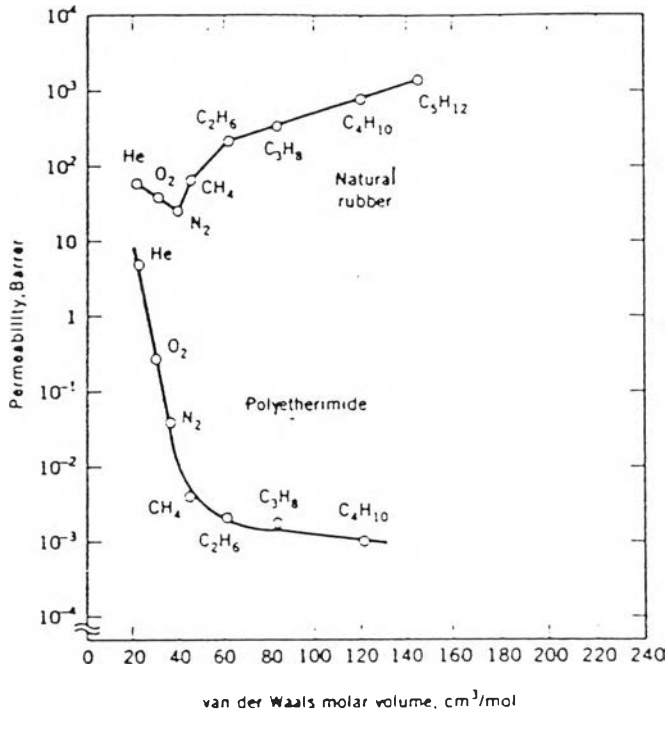

Figure 2.3 Permeability as a function of molar volume for a rubbery and glassy polymers.

2.1.1.4.1 Transport in Rubbery Polymers

Permeation in rubbery polymers above their glass-transition temperature can be described by Fick's First Law (equation 2.1). A mathematical solution for the finite solid with a constant diffusion coefficient can evaluate the total amount of permeate Q [cm^3 (STP) /cm^2] passing through the polymer from t=0 to t=t.

$$Q = \frac{DC_{i(o)}t}{l} - \frac{C_{i(l)}l}{6} \qquad (2.4)$$

Equation (2.4) shows that the amount of permeant increases linearly with t. When extrapolating back the linear portion of Q vs. t plot to the time axis, one obtains an intercept t = θ, where Q = 0 and

$$D = \frac{l^2}{6\theta} \qquad (2.5)$$

θ is the diffusion time lag and provides an experimental method for the determination of D.

The diffusion coefficient, Permeability Coefficient, and solubility constant for gases may be expressed by equations of Arrhenius form (Barrer, 1939):

$$D = D_0 \exp(-E_D /RT)$$
$$P = P_0 \exp(-E_P /RT)$$
$$S = S_0 \exp(-\Delta H_S /RT)$$

where D_0,P_0, S_0 are constants, cm^2/s, [cm^3(STP) .cm]/(cm^2.s.cmHg), and [cm^3 (STP)] /cm^3.cmHg),respectively.

E_D is activation energy for diffusion, cal/(gmol).

E_P is activation energy for permeation, cal/(gmol).

ΔH_S is heat of solution, cal/(gmol).

R is gas constant, cal/(gmol.K).

T is the absolute temperature, K.

2.1.1.4.2 Transport in Glassy Polymers

Gas sorption in glassy polymers is more complicated due to the more restricted segment motions so that these materials offer enhanced mobility selectivity as compared to rubbery polymers. Transport in glassy polymers is most often governed by penetrant size. The correlation between the diffusivity D and the physical property E_D, for glassy polymers, traditionally invoked in rubbery polymer tends to break down. The existing influence in the Arrhenius plot of D near the glass-temperature is shown in Figure 2.4. The physical characteristic of glassy polymers is the "unrelaxed " volume locked into these materials when they are quenched below the glass transition. The first occupied sorption is viewed arising from uptake into a dissolved environment similar to sorption in low molecular weight liquids and rubbery polymers, and is described by a Henry's Law relation. The second occupied sorption is viewed as being due to uptake into the unrelaxed volume or " microvoids" present in glassy polymers, which is described as a Lang-muir "hole-filling" process. Therefore, the total sorption is the sum of these two populations as follows;

$$c = c_D + c_S \tag{2.6}$$

$$c = Sp + \frac{c'_S bp}{1 + bp} \tag{2.7}$$

where S is the Henry's Law constant.

p is the penetrant pressure.

c_S' and b are the Langmuir capacity constant [cm^3 (STP) /cm^3] and affinity constant [cm^3 (STP) /cm^3], respectively.

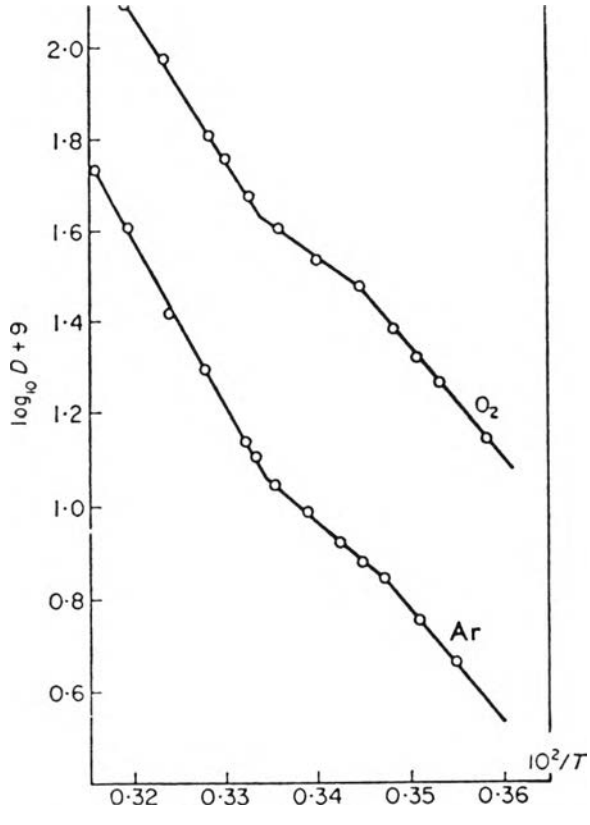

Figure 2.4 Temperature-dependence of the diffusion constants for argon and oxygen in polyvinyl acetate.

The permeation flux is expressed as:

$$N = -D_{eff} \frac{dC}{dx} \qquad (2.8)$$

where D_{eff} is the effective diffusion coefficient which is dependent on concentration. The effective diffusivity determined by low-pressure time-lag measurements corresponds to the following equation:

$$\lim_{p1\to 0}\left(\frac{l^2}{6\theta}\right) = \lim_{p1\to 0}(D_{eff}) = D\left(\frac{1+FB}{1+B}\right) \qquad (2.9)$$

where D is diffusion coefficient which is due to " dissolved " concentration component and is the only applicable diffusion coefficient above the glass-transition temperature.

F is ratio of the diffusion coefficient of the permeate in " holes" to the diffusion coefficient of the permeate in the true solution D.

$B = C'_H b/S$

p_1 is the upstream driving force.

The permeability in this dual-mode –sorption model is given by the following equation:

$$P = SD\left(1+\frac{FB}{1+bp_1}\right) \qquad (2.10)$$

According to equation (2.10), the first term determines transport in the Henry's Law environment, while the second term is related to the Langmuir environment. There is also a limit equal to SD, equation2.41, at high pressure as shown in Figure 2.5.

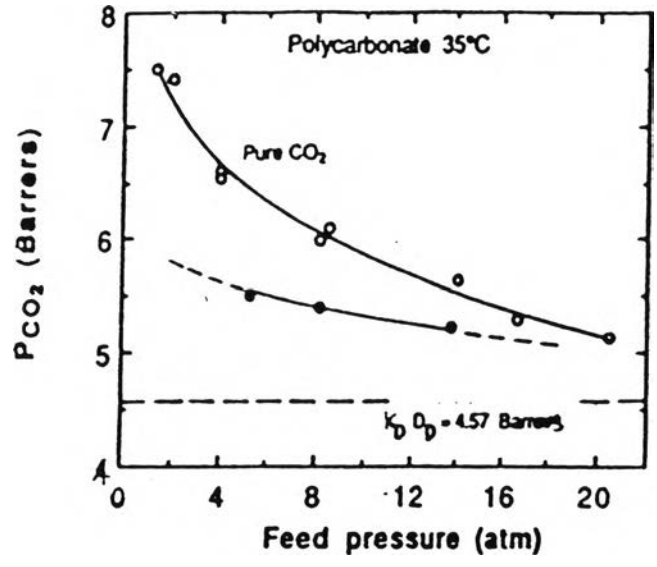

Figure 2.5 Pressure-permeability coefficients relationship of CO_2 transport in glassy polycarbonate (1 barrer = 10^{-10} cm^3(STP) cm/s cm^2 cmHg).

2.1.2 Transport by Laminates

Reciprocal permeability is an additive property when permeabilities are not dependent on pressure. This equation is applied to the great majority of laminates or barriers in series provided each of the barriers making up the laminate (including adhesive layers) which has a permeability coefficient. It should be noted that the thickness of each layer ,l_i, must be taken into account and that $l = l_1+l_2+l_3+\ldots l_n$ (He *et al.*, 1996)

2.1.3. Factors Affecting the Diffusivity of Gas

2.1.3.1 Nature of Gases

As a whole (Crank and Park, 1965), it is clear from the mechanism of the activated diffusion process that the larger holes need to be formed in the polymer for the diffusion of larger molecules and require larger

energies for large holes formation. Hence, the activation energy will be larger for the diffusion of larger molecules and the diffusivity will be smaller. Otherwise, it is found that the activation energy is composed of an intermolecular term, E_i, and an intramolecular term, E_b. The first depends upon the penetrant molecule diameter, σ_p, the average diameter of the high polymer molecule, σ_c, the dimension corresponded to the free volume per unit length of chain molecule ($\phi^{1/2}$ /2) and the segment length, S. The second is related to the penetrant molecule diameter, σ_p, the dimension corresponded to the free volume per unit length of chain molecule ($\phi^{1/2}$ /2), the segment length S, and the length of one backbone chain bond Λ measured along the chain axis. For a particular polymer, the effect of penetrant molecule diameter is dependent on the relative magnitudes of the intermolecular and intramolecular energies. For the predominance of intermolecular energy, the activation energy will vary directly with the penetrant molecule diameter whereas it will vary directly with the square of the penetrant molecular diameter for the predominance of intramolecular energy.

2.1.3.2 Nature of Polymers

From the hole theory of diffusion, the rate of diffusion will depend on

- The number and size distribution of pre-existing holes upon the ease and degree of packing of the chains and the relevant to the free volume and the density.
- The ease of hole formation will depend on the segment chain mobility, i.e. the chain stiffness, and on the cohesive energy of the polymer.
- The degree of crystallinity and of crosslinking as well as additives such as fillers and plasticizers.

The introduction of unsaturation into the polymer backbone lends greater ease of rotation to the chains leading to higher diffusivity of penetrants or greater chain flexibility of the unsaturated polymer (shown in Table 2.1).

Table 2.1 The effect of unsaturation on the diffusion of octadecane in polymers at 50 ^{0}C

Polymer	Density @ 25 ^{0}C	Dx10^{7}
Polybutadiene	0.892	3.62
Polybutadiene 92% saturated	0.894	1.40
G.R.S.rubber	0.932	2.29
G.R.S.rubber 97% saturated	0.903	1.21
Polyisoprene	0.909	3.06

The introduction of methyl groups decreases the chain flexibility and causes lower diffusion constants as well as a greater energy of the activation for diffusion. It is thought that a longer chain segment may be consistent due to steric hindrance. Similarly, in a series of amorphous ethylene-propylene copolymers, the diffusivity decreases with increasing propylene content.

The introduction of polar side-chains causing an increase in the cohesive energy of the polymers also leads to a decrease in the gases diffusivity and an increase in the activation energy.

Chain flexibility and cohesive energy also effect other properties of a polymer, such as glass temperature. In general, the glass temperature affects the diffusivities and activation energy. The glass temperature increases with decreasing diffusivities and increasing activation energy.

2.1.3.3 Effect of Glass Temperature

For an Arrhenius plot of all the studied gas diffusivities and permeability coefficients, there is a distinct change of slope at the glass transition point with a lower-energy of activation for the polymer in the glassy state. This is an indication of a less well-defined intermediate region near the glass transition point with a smaller slope than above or below it. However, there was no inflection in the Arrhenius plots of the diffusivities, nor in the permeability. In a study of the diffusion of gases through a vinyl chloride-vinyl acetate copolymer, it was found that there was no effect of the glass transition for all gases, except CO_2. Since the number of holes doesn't substantially change above the glass temperature this leads to a size of the hole changes, i.e., the amplitude of the segmental oscillations or rotation increases. If the penetrant were small enough, only minor changes would be displayed since the probability of a penetrant molecule encountering a hole would remain roughly the same. For the larger penetrant molecules, a more importance dependence of the size on the glass transition can be seen. Consequently, for the studied copolymer, CO_2 would represent the limiting size in spite of cases for polyvinyl acetate or polyethylene terephthalate, almost all the penetrants were large enough to detect this effect.

When the penetrant size is much less than the average hole size in the polymer, it is suggested that diffusion takes place by localized activated jumps from one pre-existing cavity to another. As the size of the penetrant increases or the hole size decreases, this mechanism may cease to be

dominant because of fewer available cavities to accommodate the penetrant molecule. Much larger numbers of monomer segments will thus need to be rearranged for the penetrant to pass from one cavity to another. Subsequently, this process becomes more dependent on the macroscopic free volume of the polymer. Since the rate of change of the free volume with temperature affects the changes at the glass temperature, a change in slope of the Arrhenius plots will be observed such as mentioned above for example, polyethyl methacrylate which has a large average cavity.

2.1.3.4 Effect of Crosslinking

The degree crosslinking increases, the diffusion constants decrease and the magnitude of the change is greater, the larger the penetrant molecule. In addition, the energy of activation for diffusion and the pre-exponential factor increases with increased crosslinking. Finally, the crystallinities themselves act as giant crosslinks and tend to immobilize the chains.

2.1.3.5 Effects of Plasticizers and Relative Humidity

The addition of a plasticizer to a polymer decreases the cohesive forces between the chain. As a result, it increases segmental mobility and hence increases the rate of diffusion and lowers the activation energy. The effect of relative humidity on gas diffusion in polymers varies widely. In case of low solubility of water in the polymer, less than 1 % RH, there is no effect whereas, in intermediate cases (up to 20 %), there arises a small reduction in the diffusivity in some cases and an increase in others.

2.2 Palladium - Hydrogen Diffusion and Absorption

The interaction of hydrogen with metals is fundamental to this study. The dissociative chemisorption of molecular hydrogen on transition-metal

surfaces is one of the simplest heterogeneous chemical reactions. This reaction is also important in many industrially important catalytic processes such as olefin hydrogenation, the Fisher-Tropsch process, and ammonia synthesis. Moreover, the subsequent permeation of atomic hydrogen into the bulk gives rise to such deleterious effects as hydrogen-induced embrittlement and cracking. Penetration of hydrogen into the bulk is important in the first interactions in fusion reactors and metal hydride solid-state hydrogen storage materials.

2.2.1 The Kinetic of Hydrogen Absorption in Palladium

Auer and Grabke (1974) studied the kinetics of hydrogen absorption on a Pd surface as follows,

$$H_2 = 2H(\text{dissolved}) \qquad (2.11)$$

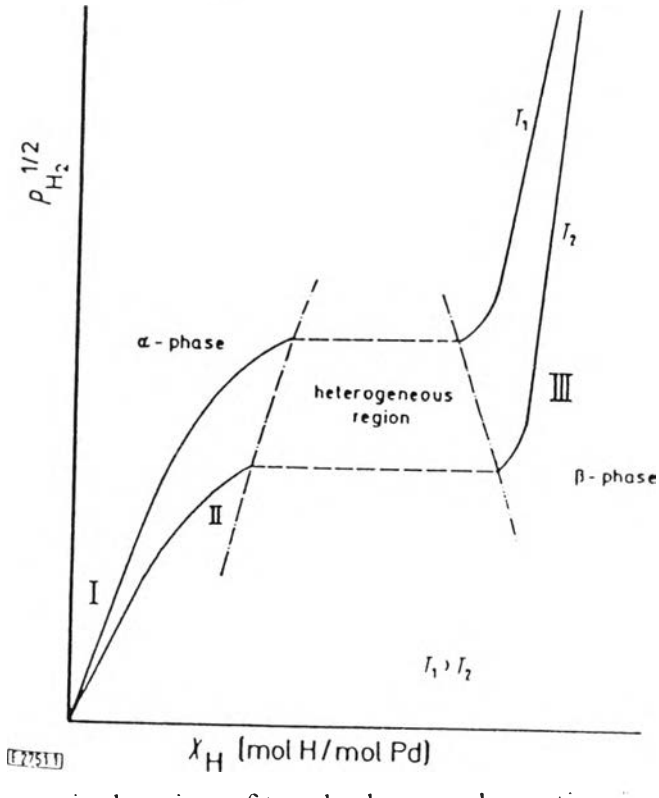

Figure 2.6 Schematic drawing of two hydrogen absorption isotherms.

Sieverts law is valid at low concentrations in Pd (region I in the schematic drawing of the isotherm, Figure 2.6).

$$P_{H2}^{1/2} = K.\, x_H$$

For region II, the transformation of the α- to β-phase is approximately given by

$$P_{H2}^{1/2} = K.x_H.\exp(Ex_H/RT)$$

In the region III in Figure 2.6 or the β-phase, the isotherm can be expressed by the empirical law;

$$\ln P_{H2}^{1/2} = -A(T) + B(T)\, .x_H$$

The rate-determining step is the dissociation of the H_2-molecule on the metal surface. It is assumed that the formation of the activated complex one atom (proton) already enters an interstitial site in the lattice. For low hydrogen concentrations x_H in the α-phase Pd and in the Pd-Ag alloy, where Sieverts law applies (Region I in Figure 2.6), the following rate law is valid.

$$v = k \frac{1}{1 + Kx_H} p_{H_2} - k' \frac{Kx_H^2}{1 + Kx_H} \qquad (2.12)$$

where k and k' are the rate constant for the forward reaction and the backward reaction, respectively K is the equilibrium constant for the adsorption equilibrium [H (dissolved) $\longleftrightarrow$ H(adsorbed)]. x_H is the mole fraction of hydrogen and p_{H2} is the hydrogen partial pressure.

According to the rate law, there is a segregation equilibrium between dissolved atoms and atoms in the interstitial reaction sites. For the α-phase Pd, the enthalpy of this segregation is –1.9 kcal/ mol H. The forward reaction and backward activation energy are 6.8 kcal and 11.5 kcal, respectively, which gives a reaction enthalpy of –4.7 kcal/mol H_2.

For the Pd-Ag alloy, in dilute solution, the activation energies obviously are in the same range, as on the Pd, 7 to 9 kcal/ mol H_2. The initial rates of the forward reaction increase with increasing silver content of the alloy.

Bucur *et al.* (1976) have proposed another model for hydrogen absorption in palladium in which both the absorption and the desorption cycles are controlled by two successive partial steps;

1. The second order step, which is respect to sorbed H and occurs in the early stages of the processes, is the dissociation of Hydrogen (Deuterium) molecules (absorption) and the recombination of the surface hydrogen (Deuterium) atom (desorption)

$$H\,(\text{adsorbed}) \leftrightarrow H\,(\text{bulk}) \qquad (2.13)$$

2. The first order step (diffusion step) was either the transfer of H atom from the surface into the bulk of Palladium or the surface migration of the hydrogen atom from one type of adsorption site to another, which becomes operative in the last stage of the process.

$$H_2(\text{gas}) \leftrightarrow 2H(\text{adsorbed}) \qquad (2.14)$$

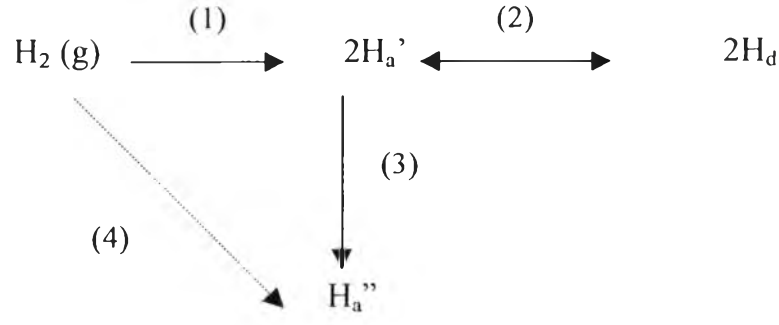

Figure 2.7 Schematical diagram of the absorption and the desorption cycles for hydrogen on palladium.

The removal of adsorbed hydrogen is more difficult and required a higher temperature. These results suggest that the sorption or removal of hydrogen in or from palladium, in both the adsorbed and absorbed states, could take place through two independent pathways with the following suggested mechanism, as shown in Figure 2.7. The dissolution of hydrogen occurs through the chemisorption step (1) and transfer step (2) until equilibrium is established between the gas phase and the dissolved hydrogen. The transfer step is faster than all the other steps and the " pre-dissolved" state H_a' is in equilibrium with the dissolved one, H_d. The surface migration step (3) starts in the last stage of the absorption process and it is the rate-determining step until complete equilibrium is obtained between the bulk hydrogen and the adsorbed species, H_a' and H_a'' (first order kinetics). Otherwise, it could be supposed that the H_2 molecule may be adsorbed directly from the gas phase, step (4), but this probability is very small because of the high energy barrier for the direct adsorption process.

On a metallurgical Pd sample having a smooth surface, the density of the H_a'' adsorption sites is small and so the contribution of the surface migration step (3) is negligible. It follows from this that during the

sorption process chemisorption is the only rate-determining step. On the other hand, on a Pd sample with a high surface – to – volume ratio (vacuum evaporation) or high active surface area (electrodeposition), the density of the H_a'' adsorption sites is high and the quantity of adsorbed hydrogen is comparable to the dissolved hydrogen. The filling-up of these adsorption sites through surface migration (3) becomes the rate-determining step for the sorption process and it operates with first-order kinetics.

Kay *et al.* (1986) have studied the interaction of hydrogen with well-characterized single-crystal Pd surfaces. The uptake rate is limited by bulk atomic diffusion rather than by dissociation chemisorption since the square-root pressure dependence of the initial absorption rate is indicative of a diffusion limited process. Similar results are obtained at other temperatures (60,80,120,and 140 °C). The diffusion coefficients determined in this study are in excellent agreement with the accepted values for bulk diffusion of hydrogen through palladium. Furthermore, their measured initial rates are between 50 and 100 times faster than those found by Auer and Grabke (1974) even though their sample is 350 times thicker. They suggested the low apparent H_2 dissociation probability may arise from uncharacterized surface contamination on their samples.

As a benchmark system for the poisoning of transition metal surfaces is the adsorption of sulphur on Pd (100) and its influence on the dissociative adsorption of H_2. Wilke and Scheffler (1995) used density functional theory in order to study the adsorption of hydrogen on clean and sulphur precovered Pd(100) surfaces. The results indicate that the poisoning effect of sulphur is not caused by a strict blocking of hydrogen adsorption sites in the vicinity of S atoms, such as for a (2x2) sulphur adlayer (coverage $\theta_S = 1/4$), hydrogen adsorption remains an exothermic process for all surface hollow sites not occupied by sulphur. The blocking of hydrogen adsorption

happens only for higher sulphur coverages resulting from the strong repulsive H-S interaction which blocks the adsorption of hydrogen in the vicinity of the sulphur adatoms.

Okuyama *et al.* (1998) have studied the path and mechanism of hydrogen absorption at Pd (100) in the temperature range (105-200°K). According to the absorption mechanism (Figure 2.7), the schematical energy variation for H atoms in the gas-phase H_2(I) on Pd (100)(II), at the subsurface sites (III), and in the Pd bulk (IV) is shown in Figure 2.8.

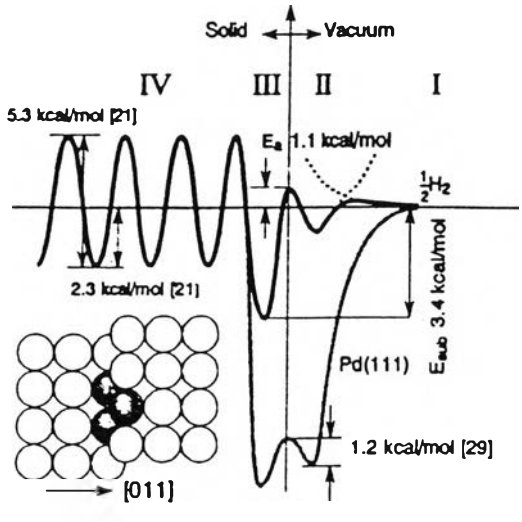

Figure 2.8 Energy diagram for H near the Pd(100) surface (solid curve).

There are three basic elementary steps to the process of absorption of H_2 by palladium.

1. dissociation on the surface (I → II)
2. penetration into the subsurface sites (II → III)
3. bulk diffusion (III → IV)

Below 120 K, H atoms penetrate via quantum tunneling and remain at the subsurface sites to form palladium hydride, which gives rise to a molecular hydrogen desorption peak at 155 K. The absorption energy for the subsurface site is estimated to be 3.4 kcal $molH^{-1}$. At higher temperatures, the hydrogen atoms diffuse thermally into the Pd bulk during exposure and desorb at around 300 K, exhibiting a broad structure. An isotope difference is observed in the absorption state which is associated with the higher mobility of D. The activation energies of penetration into the subsurface sites are determined to be 1.1 kcal $molH^{-1}$ and 0.8 kcal $molD^{-1}$.

2.2.2 Polymer – Hydrogen Diffusion

According to transport though polymeric membranes, the separation for membrane-based processes is the result of the differences in the transport rates of the chemical species through the interface (Pinto *et al.*, 1999). There are three types of mass transport through membranes: passive, facilitated, and active, which all depend on whether this occurs in favour of or against the electrochemical potential gradient of the system.

- Passive transport, the membrane acts as a barrier through which the components are transported under the effect of a gradient and their electrochemical potential gradient.

- Facilitated transport, as well as the effect of an electrochemical potential gradient, the components react with a carrier in the membrane; therefore, permeability increases considerably.
- Active transport, the permeated species can be transported against the gradient of their electrochemical potential. The driving force for transportation is produced by a chemical reaction occurring inside the membrane.

Transport through membranes is a non-equilibrium process, which is related to bulk force. These force are mainly due to difference in concentration, difference in pressure and difference in electrical potential, leading to flows of mass , of volume and of charge, respectively.

Hughes and Jiang (1995) have studied the permeabilities of CO_2, N_2O, and O_2 and their mixtures through silicone rubber and cellulose acetate membranes. For silicone rubber, N_2O had the highest permeability with CO_2, O_2, following respectively. All three gases are feed pressure independent, but there was temperature dependence of N_2O and CO_2 permeability coefficients whereas does have an effect on the O_2 permeability increasing with temperature. On the other hand, both CO_2 and N_2O permeability coefficients increase with the pressure ratio, whereas the feed pressure has no effect on the O_2 permeability coefficient in cellulose acetate membrane. A comparison of the permeability coefficients for silicone rubber and cellulose acetate was made at 100 kPa and 220 °C. It indicate that cellulose acetate gives much higher permeabilities than silicone rubber, but there is no selective separation between N_2O and CO_2 which it is probably due to their similarity in physical properties. The diameters of molecules are similar, 3.83 A° for N_2O and 3.94 A° for CO_2, and the permeability coefficients are essentially identical ($P_{CO2} = 1.326 \times 10^{-10}$, $P_{N2O} = 1.326 \times 10^{-10}$ $m^3 m\ m^{-2}\ s^{-1}\ kPa^{-1}$).

Matsuyama *et al.* (1999) have studied facilitated transport of CO_2 through polyethylenimine (PEI)/poly(vinylalcohol) (PVA) blend membrane. PEI/PVA blend membranes were prepared and the facilitated transport of CO_2 was investigated since the CO_2 permeance decreased with the increase in the CO_2 partial pressure, whereas the N_2 permeance was nearly constant. In addition, PEI functioned efficiently as the carrier of CO_2. The PEI wt % effect in the blend membrane on the permeability and the selectivity was investigated. The CO_2 and N_2 permeabilities increased monotonically with increasing PEI wt % because the membrane become more swollen at the condition of the higher PEI wt %.

For composite membranes, an improved resistance model based on Henis-Tripodi's model for gas permeation in composite membrane has been established. The effects of the degree of penetration, the thickness of the coating layer, the surface porosity of the dense layer, and the separation factor of the composite membrane have been studied. They found that the degree of penetration has an important effect on the membrane separation properties. It is recommended that making the degree of penetration greater than 0.4 will provide high selective composite membranes. The greater degree of penetration, the higher separation factor will not decrease the permeation flux of the composite membrane. The thickness of the coating layer is very important for controlling the degree of penetration and the thickness of the coating layer .The deeper the coating materials penetrate into the pores the thinner the thickness of coating layer, the higher the membrane separation. The effect of porosity is an important with a smaller porosity (ε), giving a larger degree of penetration.

Oh and Zurawsky (1996) have examined the basic transport properties of plasma polymer/dense polymer composite membranes and determined whether the properties of the plasma polymer coatings are similar

to those on porous polymer substrates, and whether the properties of the composites can be sufficiently defined from a simple resistance in series model. They found that the permeation properties of the plasma polymer films on dense polymer substrates is the same as those of the plasma polymer films on porous substrates when coating on the dense polymer substrate are thicker than about 0.12 μm. The permeabilities of the composites depend linearly on the thickness of the plasma polymer coating and the composite properties. For O_2 and CO_2 permeation, the composites behave ideally within experimental error, whereas, for N_2 and CH_4, both deviate from the simple resistance in series model, which has the additional resistance to permeation due to plasma modification of the PDMS substrate. CH_4 indicates the largest deviation from the resistance in series model. This may be due to the largest of the tested permeates. The additional or interfacial resistance arises as an Arrhenius temperature dependence.

Inorganic membranes have recently been investigated due to their unique properties: good thermal, chemical and structure stability, long life in application and ability of having catalytic and electrical properties. The microporous inorganic membrane is governed by the Knudsen diffusion mechanism (Chai *et al.*, 1994). This kind of membrane was prepared for selective separation of hydrogen using the sol-gel method. It was found that the permeability of hydrogen and the separation factor for the gaseous hydrogen/nitrogen mixture using metal-dispersed membranes, such as Ru-, Rh-, Pd-, Ni-, and Pt-Al_2O_3 membranes exceeded the expected value for Knudsen diffusion. Therefore, although the gas permeation through the alumina membrane was governed by Knudsen diffusion, the metal particles dispersed in the alumina membranes affected the hydrogen permeation. Otherwise, the separation factors of the Rh-, Ru-, Pd-, Pt- and Ni- for dispersed alumina membranes increased with increasing temperature, as did the permselectivity.

Asymmetric molecular sieve carbon membranes were studied by Shusen *et al.* (1996). There were formed by conventional pyrolysis of a thermosetting polymeric film, followed by unequal oxidation. The molecular sieve carbon membrane is rapidly developing due to its excellent characteristics for gas separation as compared with polymeric membranes. Experimental results indicate that thickness and pore size of the ceramic sheet exert an important effect on the membrane properties. Hence, Knudsen diffusion can separate gases according to their molecular weight. With regard to the kinetic theory, the lighter gases are expected to diffuse faster in the Knudsen diffusion regime. Table 2.2 indicates that this is not always the case. Consequently, Knudsen diffusion cannot explain the experimental results in Table 2.2.

Table 2.2 Pure gas permeabilities of a typical asymmetric carbon membrane (unit Barrer)[(a)]

Membrane Type	H_2	O_2	N_2
Silicone rubber membrane	520	396	184
Symmetric carbon membrane		1710	240
Asymmetric carbon membrane	5100	2300	216

(a) 1 Barrer is 10^{-10} cm^3(STP) cm/s cm^2cmHg

The remaining feasible controlling mechanism is molecular sieving. Molecular sieves are porous membranes that contain pores of molecular dimensions which can exhibit selectivity due to the size of the molecule. The permeability of gases through the asymmetric carbon membrane appears to be related to their kinetic diameter supporting the molecular sieving mechanism (see Table2.3).

Table 2.3 Molecular weight and kinetic diameter of feed gases

Gas	Kinetic diameter (nm)	Molecular weight (g/mol)
H_2	0.297	2.0
O_2	0.354	32.0
N_2	0.375	28.0